Available online at www.sciencedirect.com
ScienceDirect
Bioorganic & Medicinal Chemistry 15 (2007) 4406–4418
Bioorganic & Medicinal Chemistry

Synthesis of analogues of a flexible thiopyrylium photosensitizer for purging blood-borne pathogens and binding mode and affinity studies of their complexes with DNA

Ruel E. McKnight,[a,*] Mao Ye,[b] Tymish Y. Ohulchanskyy,[b] Sadia Sahabi,[a] Bryan R. Wetzel,[b] Stephen J. Wagner,[c] Andrey Skripchenko[c] and Michael R. Detty[b,*]

[a]*Department of Chemistry, State University of New York at Geneseo, 1 College Circle, Geneseo, NY 14454, USA*
[b]*Institute for Lasers, Photonics, and Biophotonics, Department of Chemistry, University at Buffalo, The State University of New York, Buffalo, NY 14260, USA*
[c]*American Red Cross, Holland Laboratory for the Biomedical Sciences, 15601 Crabbs Branch Way, Rockville, MD 20855, USA*

Received 14 February 2007; revised 16 April 2007; accepted 18 April 2007
Available online 25 April 2007

Abstract—A series of thio- and selenopyrylium analogues of 2,4-di(4-dimethylaminophen-yl)-6-methylthiopyrylium iodide were prepared in five steps from 4-dimethylaminophenyl-propargyl aldehyde and the corresponding lithium acetylide. When bound to DNA, all of the dyes absorb at wavelengths >600 nm, which avoids the hemoglobin band I maximum at 575 nm. The binding of the series of dyes to double-stranded DNA was examined spectrophotometrically and by isothermal titration calorimetry to determine binding constants, by a topoisomerase I DNA unwinding assay, by competition dialysis with $[poly(dGdC)]_2$ and $[poly(dAdT)]_2$, and by ethidium bromide displacement studies to examine propensities for intercalation, and by circular dichroism studies. The dyes were found to show mixed binding modes.

1. Introduction

While the blood supply is in general safe, there remains a small residual risk of pathogen transmission via blood transfusion. If the blood is collected from an infected donor during the 'window period,' or before the individual develops detectable levels of antigen, antibody, and/or nucleic acid, then there may be no means to ascertain that the blood bears the pathogen. Among the viral pathogens of concern are hepatitis B virus, hepatitis C virus, human T-lymphotropic virus-1 and -2, and human immunodeficiency virus (HIV).[1] It is also possible that unknown transfusion–transmissible agents, like West Nile virus in 2002, will continue to emerge in the future. Thus, pathogen reduction methods have been investigated in cellular blood components to eliminate the residual risk from known organisms that are currently being screened in the blood supply and diminish the risk from unknown or emerging agents whose tests may not be available, licensed or implemented.

Photodynamic inactivation of viral pathogens in red blood cells (RBC's) and in blood components has been investigated over the past 15 years.[2] Optimal properties of a photosensitizer for *ex-vivo* decontamination of blood pathogens from blood include selection of dyes that (1) have high chemical purity and known composition, (2) are capable of inactivating both intracellular and extracellular pathogens, (3) have a high affinity for pathogens relative to red cells to facilitate pathogen photoinactivation with limited damage to red cells, (4) absorb light in a spectral region where light attenuation by hemoglobin absorption (λ_{max} of 413, 541, and 575 nm) is avoided, and (5) display little dark toxicity toward either red cells or transfusion recipients. One means to target viral pathogens is to select photosensitizers that bind to viral DNA or RNA, since red blood cells do not contain nucleic acids.

Keywords: Chalcogenopyrylium dyes; DNA-binding; Topoisomerase I unwinding assay; Competition dialysis; Ethidium displacement; Circular dichroism.
* Corresponding authors. Tel.: +1 585 245 5451; fax: +1 585 245 5288 (R.E.M.), Tel.: +1 716 645 6800x2200; fax: +1 716 645 6963 (M.R.D.); e-mail addresses: mcknight@geneseo.edu; mdetty@buffalo.edu

0968-0896/$ - see front matter © 2007 Elsevier Ltd. All rights reserved.
doi:10.1016/j.bmc.2007.04.033

Methylene blue (MB), methylene violet (MV), and dimethylmethylene blue (DMMB) have been extensively investigated for pathogen reduction in red cell suspensions.[3] One advantage of these dyes is their association with nucleic acids,[4–8] suggesting that these photosensitizers would be more specific for pathogen reduction and cause less damage to red cells. MB is currently being used for the decontamination of freshly frozen plasma units.[3] However, despite this successful application to plasma, all early attempts to develop photosensitizers for pathogen inactivation of RBC's have failed, either because of poor virucidal activity in blood or because of excessive hemolysis during storage.

The pyrylium dyes **1-O** and **2-O** and the thiopyrylium dyes **1-S** and **2-S** (Scheme 1) have been described as intercalators of double-stranded DNA.[9] Binding of these analogues to DNA was accompanied by a bathochromic shift in the absorption maximum of each dye and 18- and 32-fold increase in fluorescence intensity for **1-O** and **1-S**, respectively, and 400- and 100-fold increase in fluorescence intensity for **2-O** and **2-S**, respectively, relative to the unbound dyes in solution. The thiopyrylium dye **2-S** is useful for the photochemical reduction of viral and bacterial pathogens in RBC's presumably due to changes in the dye's photophysical properties upon binding to nucleic acids (increased relative yields of *both* fluorescence *and* triplet/singlet-oxygen generation).[10] However, high concentrations of **2-S** (1.0×10^{-4} M) were required to achieve these results and hemolysis was still an issue that needed to be addressed through the use of a storage medium that protects against colloidal osmotic hemolysis and the use of a competitive inhibitor for dye binding to red cells.

Because of these encouraging preliminary results with **2-S** as a photosensitizer for inactivation of viral and bacterial pathogens in RBC's,[10] we have prepared a series of analogues for further study. Herein, we describe the synthesis of these analogues and their binding to DNA via changes in absorption spectra, the determination of binding constants with spectrophotometric titration and isothermal titration calorimetry (ITC), a topoisomerase I DNA unwinding assay (Topo I assay), competition dialysis experiments with $[poly(dAdT)]_2$ and $[poly(dGdC)]_2$, ethidium displacement studies, and circular dichroism (CD) studies.

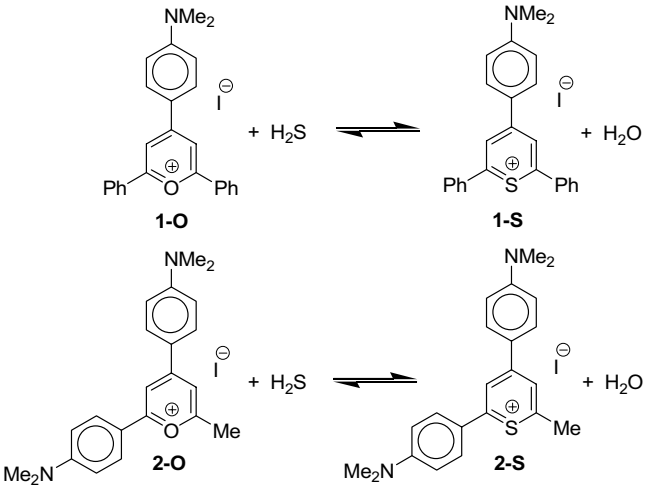

Scheme 1.

2. Results and discussion

2.1. Synthesis of dyes

The classical synthesis of the thiopyrylium analogues **1-S** and **2-S** is via the addition of H_2S[10,11] to the corresponding pyrylium dye.[12] This process is reversible as shown in Scheme 1 and mixtures of pyrylium and thiopyrylium dyes are almost always obtained. In our hands, the addition of H_2S to pyrylium dye **1-O** gave **1-S** contaminated with 5% **1-O**. In the case of **2-S**, the pyrylium contaminant **2-O** is 10% of the dye mixture and it is not possible to separate the pyrylium impurity from the desired thiopyrylium analogue **2-S**.[10] As a consequence, the photophysical and biological properties reported for the thiopyrylium analogues **1-S** and **2-S** always have contributions from the corresponding pyrylium impurity.

In earlier work, we described a synthetic route to **1-S** as well as the corresponding seleno- and telluropyrylium analogues that avoided the exchange of two chalcogen atoms to generate the desired dye.[13] The chalcogen atom is introduced via the addition of a disodium chalcogenide to 1,5-diphenyl-2,4-pentadiyn-3-one to give the corresponding chalcogenopyranone. Dyes are then generated via the addition of a Grignard reagent to the chalcogenopyranone followed by acid-induced dehydration to give the corresponding dye. This strategy allows **1-S** and analogues to be prepared free from contamination by **1-O**.

We use a similar approach to prepare a series of analogues of **2-S** as shown in Scheme 2. The addition of a lithio alkyne to 4-dimethylaminophenylpropargyl aldehyde (**3**)[14] gave the corresponding 5-alkyl-1-(4-dimethylaminophenyl)-1,4-pentadiyn-3-ols **4** in 80–88% isolated yield. The diynols **4** were oxidized to the diynones **5** in 77–87% isolated yield with MnO_2 in anhydrous dichloromethane at reflux.

The conversion of the diynones **5** to the corresponding chalcogenopyranones **6–11** required two steps. In the first step, one equivalent of EtOH was added across one of the triple bonds of the diynone to give a mixture of ethoxyeneynes as shown in Scheme 2.[15] The ethoxyeneynes are the precursors to the corresponding chalcogenopyranones. The initial addition of Na_2S or Na_2Se as a nucleophile occurs at the triple bond of the ethoxyeneynes followed by an addition/elimination reaction at the double bond to give the corresponding chalcogenopyranones **6–11** in 45–81% isolated yield. This procedure avoids the exo-cyclization to give the five-membered ring instead of the six. The addition of 4-dimethylaminophenyl magnesium bromide to **6–11** followed by acid-induced dehydration with 10%

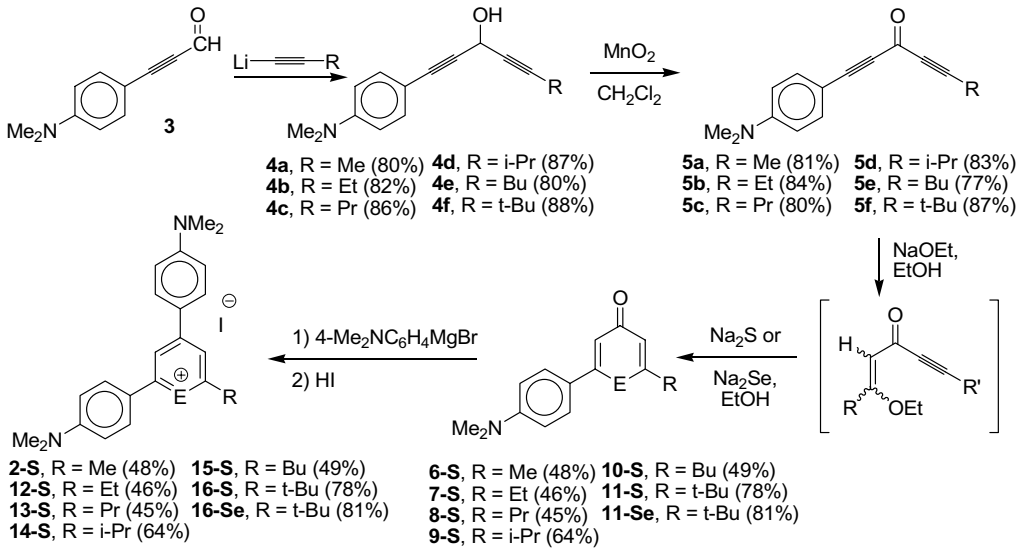

Scheme 2.

aqueous HI gave the corresponding chalcogenopyrylium iodides **2-S**, (**12-S**)–(**16-S**), and **16-Se** in 45–81% isolated yield.

The thiopyrylium dyes **2-S** and (**12-S**)–(**16-S**) and the selenopyrylium dye **16-Se** prepared by this method contained no pyrylium impurity. The iodide salt of **16-Se** was somewhat hygroscopic and was converted to the corresponding chloride salt with an ion exchange resin to give a suitable salt for elemental analysis.

2.2. Properties of chalcogenopyrylium dyes

The absorption spectra of the chalcogenopyrylium dyes **2-S**, **16-S**, and **16-Se** in water are shown in Figure 1. While the selenopyrylium dye **16-Se** has an absorption maximum near 600 nm, the thiopyrylium analogues absorb with maxima near 575 nm, which overlap the band I absorption maximum of hemoglobin at 575 nm. However, upon complexation to calf thymus DNA (ctDNA), a 30–40-nm bathochromic shift is observed as well as an increase in the molar extinction coefficient (Fig. 1). When DNA-bound, all of the chalcogenopyrylium dyes have absorption maxima at wavelengths >600 nm, which provides an appropriate window for photoinactivation of blood-borne pathogens while avoiding the hemoglobin band I maximum at 575 nm.

Values of the *n*-octanol/water partition coefficient were measured for the chalcogenopyrylium dyes and are compiled in Table 1. Values fall in the range 0.13 (for **12-S**) to 1.63 (for **15-S**). While the general trend observed is that increasing the size of the alkyl substituent gave an increase in $\log P$, the ethyl-substituted derivative **12-S** had the lowest value of $\log P$ and was lower than $\log P$ for the methyl-substituted derivative **2-S** by 0.47. The introduction of further branching in the isopropyl-substituted derivative **14-S** gave $\log P$ of 0.23, which was 0.59 smaller than the *n*-propyl-substituted derivative **13-S** and 0.37 smaller than the methyl-substituted derivative **2-S**.

2.3. Binding constants of chalcogenopyrylium dyes to DNA

Binding constants, K_b, for the dyes to DNA were determined by spectrophotometric titration using covalently closed supercoiled doubled-stranded DNA (using the genome from M13mp19) and ctDNA. Values are

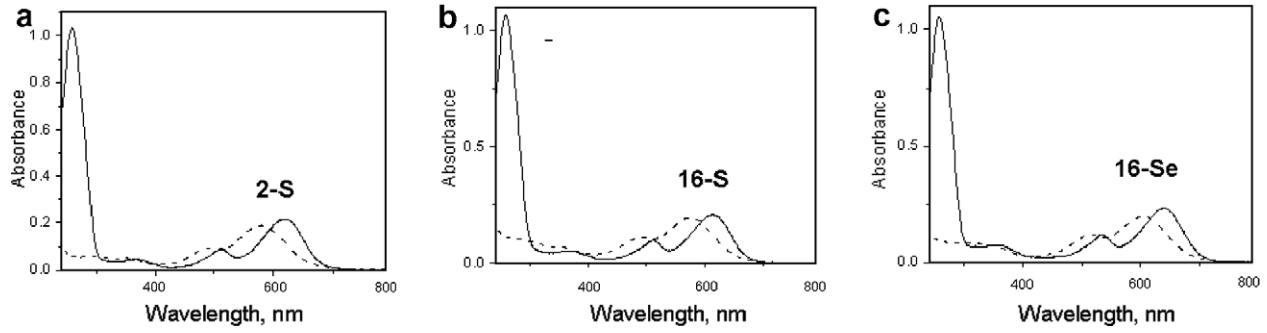

Figure 1. Spectral shifts and increased molar extinction coefficients associated with chalcogenopyrylium dyes upon binding to ctDNA. Dashed lines are dye only (8×10^{-6} M) in 0.05 M Tris–HCl, pH 7.5. Solid lines are dye (8×10^{-6} M) plus DNA (8×10^{-5} M bp) in 0.05 M Tris–HCl, pH 7.5.

Table 1. Values of the *n*-octanol/water partition coefficient (log *P*), DNA-binding affinity data (K_b), and concentrations for complete re-supercoiling in a topoisomerase I DNA unwinding assay (Topo I assay) for the chalcogenopyrylium dyes

Compound	log *P*[a]	K_b (M13mp19) (10^4 M^{-1}) (Spec. tit.)[b]	K_b (ctDNA) (10^4 M^{-1}) (Spec. tit.)[c]	K_b (ctDNA) (10^5 M^{-1}) (ITC)[d]	Topo I assay (10^{-6} M)[e]
2-S	0.60 ± 0.09	6.1 ± 0.3	5.2 ± 0.4	1.7 ± 0.4	66
12-S	0.13 ± 0.07	1.8 ± 0.1	—	—	—
13-S	0.82 ± 0.07	3.47 ± 0.06	5.0 ± 0.1	2.4 ± 0.4	45
14-S	0.23 ± 0.05	1.17 ± 0.04	—	—	—
15-S	1.63 ± 0.06	7.58 ± 0.09	—	—	—
16-S	1.51 ± 0.16	0.91 ± 0.05	10.1 ± 0.7	4.2 ± 0.6	23
16-Se	1.57 ± 0.11	2.5 ± 0.2	8.7 ± 0.4	3.9 ± 0.5	22

[a] Values are ±standard deviation.
[b] Tris buffer (0.010 M), pH 7.4.
[c] Na_2HPO_4 buffer (0.008 M), pH 7.0. Values are ±standard deviation.
[d] MES00 buffer, pH 6.25. Values are ±standard deviation.
[e] Minimum concentration of compound required for complete re-supercoiling.

compiled in Table 1. In the thiopyrylium series, values of K_b with M13mp19 DNA for the methyl (**2-S**), ethyl (**12-S**), *n*-propyl (**13-S**), and *n*-butyl (**15-S**) derivatives were larger than the thiopyrylium derivatives with branched isopropyl (**14-S**) and *tert*-butyl (**16-S**) substituents. The selenopyrylium derivative **16-Se** showed somewhat stronger binding K_b of $[(2.5 \pm 0.02) \times 10^4\ M^{-1}]$ relative to its thiopyrylium analogue **16-S** $[(0.91 \pm 0.05) \times 10^4\ M^{-1}]$. With ctDNA, the smallest values of K_b were observed with the unbranched **2-S** $[(5.2 \pm 0.4) \times 10^4\ M^{-1}]$ and **13-S** $[(5.0 \pm 0.1) \times 10^4\ M^{-1}]$ and larger values were observed with the *tert*-butyl-substituted **16-S** $[(10.1 \pm 0.7) \times 10^4\ M^{-1}]$ and **16-Se** $[(8.7 \pm 0.4) \times 10^4\ M^{-1}]$.

Binding constants (Table 1) were also measured by ITC for **2-S**, **13-S**, **16-S**, and **16-Se** with ctDNA. Figure 2 shows representative ITC data for the thiopyrylium compounds. As was seen in the spectrophotometric titration studies using ctDNA, the strongest binding affinity was observed with **16-S** [K_b of $(4.2 \pm 0.6) \times 10^5\ M^{-1}$] and **16-Se** [$K_b$ of $(3.9 \pm 0.5) \times 10^5\ M^{-1}$], while the weakest binding was observed with **2-S** [K_b of $(1.7 \pm 0.4) \times 10^5\ M^{-1}$]. Using fluorescence data and data from ITC, a size of binding site (*n*) was determined for **2-S**, **13-S**, and **16-S** to be between 3 and 4.

It is worth noting that on average the binding constants obtained from ITC were generally 3- to 5-fold higher than those obtained with ctDNA and roughly 3- to 15-fold higher than those obtained with M13mp19 DNA using spectrophotometric titration. This is presumably due to differential salt effects. The ionic strength ($[Na^+]$) used in the spectrophotometric titration was either 0.10 M (M13mp19) or 0.185 M (ctDNA) as compared to $<10^{-2}$ M in the ITC studies. It has been known for a long time now that polyelectrolyte effects can lead to significant differences in the extent of ligand–DNA interactions, especially for positively charged ligands.[16] In fact, there is usually a linear dependence between binding constant and salt concentration.

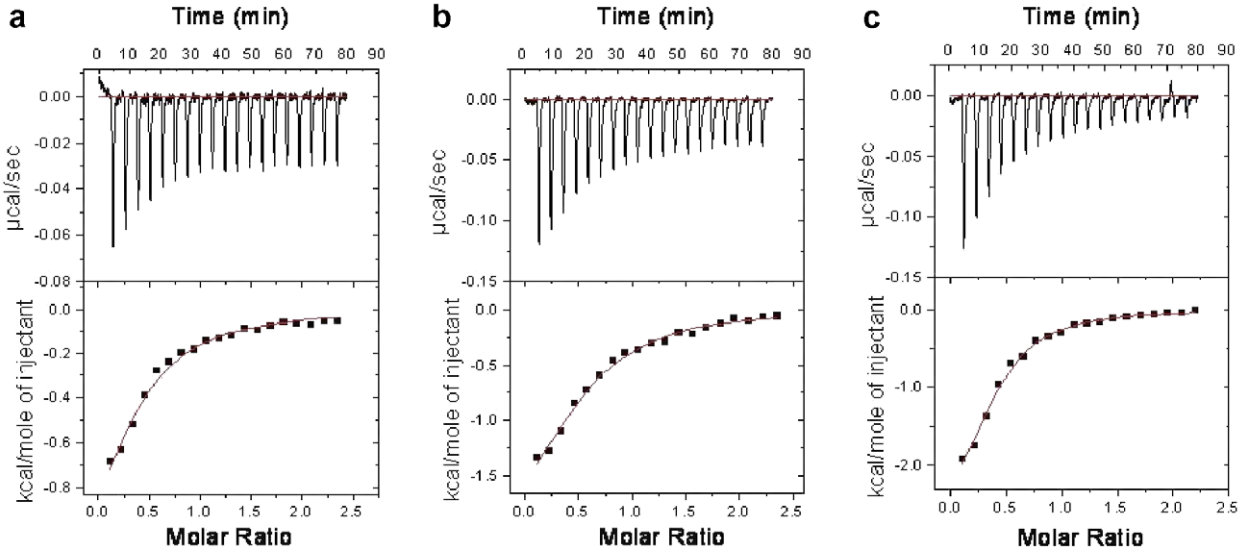

Figure 2. Calorimetric data (raw) for the titration of 1.6×10^{-4} M (a) **2-S**, (b) **13-S**, and (c) **16-S** into ctDNA (1.5×10^{-5} M in bp) at 25 °C (top). Binding isotherm (heat change vs drug/DNA molar ratio) was obtained from the integration of raw data and fitted to a 'one-site' binding model (bottom).

Binding of a charged ligand to DNA usually results in the release of condensed counterions due to (1) displacement of the cationic counterions by the positively charged ligand upon binding to DNA, and (2) for intercalators, decreases in charge density as the phosphates separate to form the intercalation site. For this reason, the effect for intercalators is usually greater than that observed for groove binders. Counterion release usually contributes favorably to the overall binding free energy change. However, this contribution decreases with an increase in the competing salt concentration leading to lower binding constants.

The values of K_b do not appear to be a function of log P for the chalcogenopyrylium dyes. With M13mp19 DNA, values of K_b appear to be 2- to 7-fold higher for derivatives with higher values of log P until one considers **16-S** and **16-Se** with the highest values of log P. Both **16-S** and **16-Se** have values of K_b more similar to **12-S** and **14-S** with the lowest values of log P. With ctDNA, a difference in log P values of 1.28 among **2-S**, **13-S**, **16-S**, and **16-Se** corresponds to values of K_b that differ by a factor of only two suggesting little correlation with log P.

2.4. Topoisomerase I studies with chalcogenopyrylium dyes

The Topo I assay exploits the ability of topoisomerase I to relax supercoiled DNA.[17,18] Under the conditions of the assay, plasmid DNA is first relaxed by the topoisomerase I enzyme and then is exposed to the compounds of the study. After removal of the compound and enzyme, intercalators will cause re-supercoiling of the plasmid DNA. Re-supercoiling is due to the change in DNA linking number that accompanies relaxation by the enzyme and occurs to the extent to which the intercalator molecule was bound.[17,19] Initial DNA unwinding will only be dependent upon the extent to which binding occurs and the minimum concentration needed to cause complete re-supercoiling will be indicative of how much compound was initially bound and the relative binding affinity. Conversely, compounds that bind solely to the DNA minor groove should not induce re-supercoiling due to negligible DNA unwinding upon binding. Results of the Topo I assay for dyes **2-S**, **13-S**, and **16-S**, and **16-Se** are shown in Figure 3 and minimal concentrations required for complete re-supercoiling are listed in Table 1 for these compounds.

The thiopyrylium and selenopyrylium compounds studied using Topo I assays caused re-supercoiling of the plasmid DNA, consistent with the involvement of an intercalative binding mode. Within the thiopyrylium series, **2-S** caused complete re-supercoiling at a concentration of 6.6×10^{-5} M which is ~3 times higher than that required by **16-S** (2.3×10^{-5} M), consistent with a ~3-fold stronger DNA affinity for **16-S**. Compound **13-S** exhibited intermediate DNA-binding affinity causing complete re-supercoiling at 4.5×10^{-5} M. Compound **16-Se** was essentially identical to its thiopyrylium analogue **16-S** with 2.2×10^{-5} M **16-Se** required to elicit complete re-supercoiling. These results suggest a 3-fold

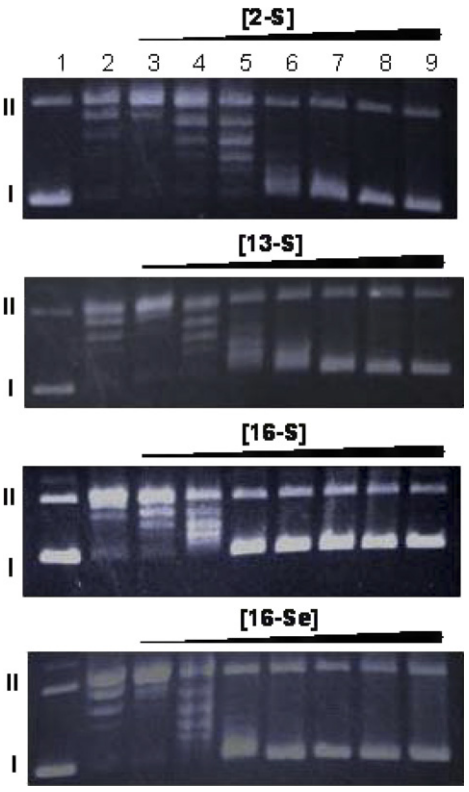

Figure 3. Topo I assay of **2-S**, **13-S**, **16-S**, and **16-Se** using 5 U of Topo I. Lane 1 contains only DNA and serves as a control. Lane 2 contains DNA and Topo I, but no compound. Remaining lanes (3–9) contain DNA, Topo I, and increasing concentrations of each compound (5–90×10^{-6} M).

range of binding affinities in the following order: **16-S** ≈ **16-Se** > **13-S** > **2-S**. This is very similar to the trend observed in values of K_b among the same group of dyes with ctDNA by either spectrophotometric or ITC methods.

These results can be compared with those described for a naphthalene diimide **17** with a similar binding constants to **16-S** and **16-Se** as measured by either ITC (5.7×10^5 M^{-1} for **17**) or spectrophotometric (1.0×10^5 M^{-1} for **17**) methods with ctDNA.[19] If the extent of intercalation/unwinding were comparable, as well, then similar concentrations of compound should give complete re-supercoiling in the Topo I assay. With **17**, complete re-supercoiling was observed at 5×10^{-6} M **17**, which is a factor of 4 less than the 2×10^{-5} M concentrations required with **16-S** and **16-Se**. Since values of K_b are similar for **16-S**, **16-Se**, and **17**, the Topo I assay results suggest that the two chalcogenopyrylium dyes have less intercalative binding than **17** (and suggests that other modes of binding may be involved).

2.5. Competition dialysis experiments

In order to differentiate preferences for intercalation and/or groove binding, the binding of the chalcogenopyrylium dyes of this study to $[poly(dAdT)]_2$ and $[poly(dGdC)]_2$ was next examined by competition dialysis. Chaires and coworkers have carried out systematic

competition dialysis studies to establish that known groove binding compounds (e.g., distamycin, berenil, and DAPI) show a strong preference (an order of magnitude or greater) for binding to $[poly(dAdT)]_2$ relative to $[poly(dGdC)]_2$.[20] The lower affinity for GC-rich sequences shown by groove binders is largely due to their restricted access to the minor groove of GC sequences caused by the protruding 2-NH_2 group of guanine. Intercalators are only expected to be affected by this if a substituent is placed into the minor groove during formation of the intercalation complex. Competition dialysis offers a direct and unambiguous approach to examine a preference for AT versus GC sequences and an implied minor groove versus intercalative mode determination, respectively.[20] In the competition dialysis approach, identical concentrations and volumes of each DNA sequence is dialyzed against a common dye solution. The system is then allowed to reach equilibrium and the concentration of dye bound to each DNA sequence determined. The relative concentrations of dye bound to each sequence give a direct measure of binding preferences.

The binding of the dyes **2-S**, **13-S**, **16-S**, and **16-Se** to $[poly(dAdT)]_2$ and $[poly(dGdC)]_2$ was examined by competition dialysis as shown in Figure 4. Compounds **2-S** and **13-S** bound to $[poly(dAdT)]_2$ with approximately 1.3× and 1.2× greater affinity, respectively, than to $[poly(dGdC)]_2$. In contrast, compounds **16-S** and **16-Se** showed 6× and 10× greater affinity, respectively, for $[poly(dAdT)]_2$ relative to $[poly(dGdC)]_2$. The results for **2-S** and **13-S** are consistent with an intercalative binding mode since no significant AT-sequence selectivity was observed. Although the results for **16-S** and **16-Se** could suggest that these dyes have more of a tendency for groove binding relative to **2-S** and **13-S**, it could also be explained by a higher intercalative affinity for the AT-rich sequence as compared to the GC sequence. In the latter case, the binding of **16-S** and **16-Se** to the GC-rich sequence would be less favorable presumably due to the protruding 2-NH_2 group of guanine into the minor groove, thus making placement of the bulky *tert*-butyl substituent in the minor groove more difficult.[21]

2.6. Ethidium bromide displacement studies

The displacement of ethidium bromide (ETBr) from ctDNA by **2-S**, **13-S**, and **16-S** was also examined in order to evaluate intercalation by the chalcogenopyrylium dyes in this study. Our ETBr displacement assays indicated that each of the thiopyrylium dyes studied caused significant decreases in ETBr fluorescence (nearly all of the ETBr fluorescence by **2-S** as shown in Fig. 5), presumably due to the displacement of ETBr from its intercalation sites.[22] Although, this is consistent with the involvement of an intercalative binding mode for the dyes as they compete with and displace ETBr from the available intercalation sites, it does not exclude the involvement of additional binding modes. It is worth noting that more than twice as much **16-S** was required to cause the same amount of fluorescence decrease as compared to either **2-S** or **13-S**. Given that **16-S** shows higher overall affinity for calf thymus DNA than **2-S** and **13-S** by either ITC or spectrophotometric titration data (Table 1), this could imply that **16-S** binds to the DNA via one or more additional modes.

2.7. Circular dichroism studies

Additional insight into the chalcogenopyrylium dye-DNA binding comes from circular dichroism (CD) measurements. The dyes of this study are achiral and do not manifest optical activity in the free, unbound state. However, when **2-S**, **13-S**, and **16-S** bind to ctDNA, all three dyes demonstrated an induced CD[23] as shown in Figure 6. The bisignate (+/−) CD observed with these dyes has several possible explanations. The bisignate behavior can be associated with an exciton interaction or two different binding sites that give different CD signals.[23] However, the low dye:base pair ratios used in our experiments and an absence of any indication of a dye–dye interaction in either absorbance or fluorescence

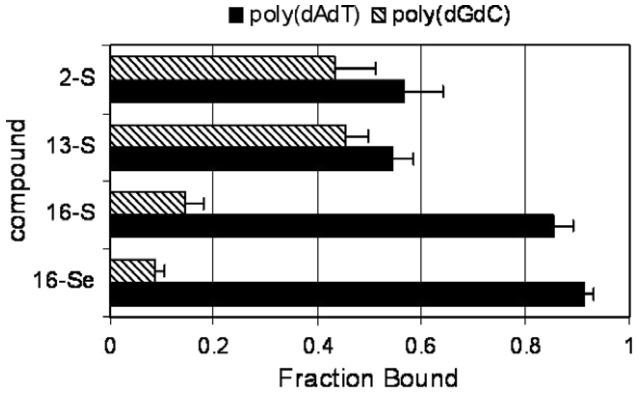

Figure 4. Fraction of **2-S**, **13-S**, **16-S**, and **16-Se** bound to $[poly(dAdT)]_2$ and $[poly(dGdC)]_2$ DNA sequences as determined by competition dialysis. In each case, the compound was dialyzed for 24 h in 0.05 M sodium phosphate buffer, pH 7.0, at room temperature. Error bars represent ±deviation from the average of duplicate runs.

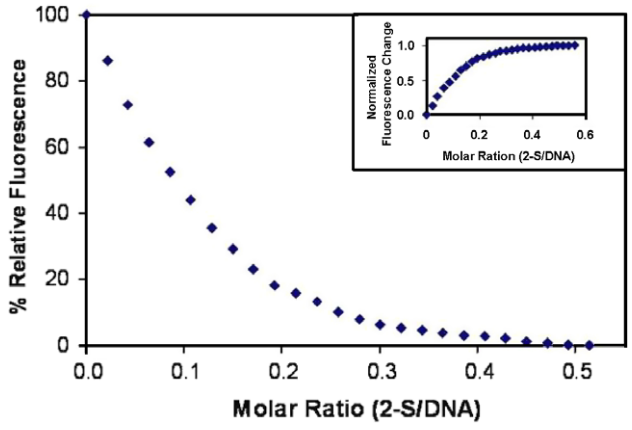

Figure 5. Fluorescence titration (ETBr displacement assay) of **2-S** (1×10^{-4} M) into ctDNA (1×10^{-5} M in bp). % Relative fluorescence is calculated based on DNA-bound EtBr (100%) and unbound ETBr (0%). The inset shows the corresponding DNA-binding curve for **2-S** based on the change in ETBr fluorescence.

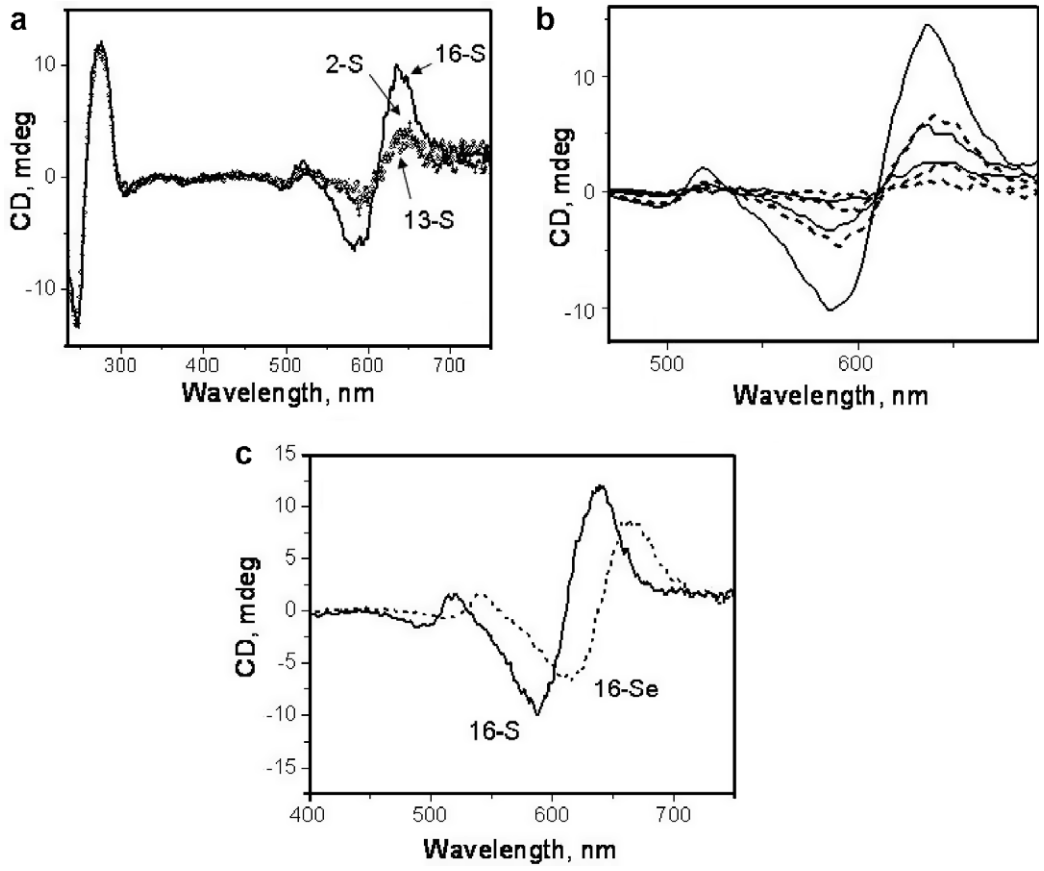

Figure 6. CD spectra of dyes complexed with ctDNA (8×10^{-5} M bp) in 0.05 M Tris–HCl, pH 7.5. (a) **2-S**, **13-S**, and **16-S** at 8×10^{-6} M dye. (b) **2-S** (dashed line) and **16-S** (solid line) at 4×10^{-6} M, 8×10^{-6} M, and 1.6×10^{-5} M dye. (c) **16-S** (solid line) and **16-Se** (dashed line) at 1.6×10^{-5} M dye.

spectra, suggest that exciton interaction between dye molecules is not responsible for the biphasic behavior for the CD spectra.

Alternatively, the bisignate CD might arise from the concurrent occupancy of two different sites in the DNA with different signs and shifts.[24] The CD spectra were acquired at different concentrations of dye (4×10^{-6}–1.6×10^{-5} M) with a constant concentration of bp (8×10^{-5} M). Although the intensity of the CD signal increased, the shape of the spectrum is unchanged, which suggests that the dye binding mode or the ratio of binding modes (intercalation vs groove binding) is unchanged with increased concentrations of dye (Figure 6b).

One explanation for the bisignate behavior is that the dye is equally likely to bind 'head-to-head' or 'head-to-tail' with DNA in the minor groove and that these orientations have different signs and shifts. Increasing dye concentrations would still populate both orientations equally. Another plausible explanation for the bisignate behavior is the lateral displacement of an intercalated dye molecule from the central helix axis with the magnitude of the CD signal determined by the extent of the lateral displacement of the dye.[24,25] One can attribute the higher intensity of the CD spectrum of **16-S** and **16-Se** at a given dye concentration relative to **2-S** or **13-S** to the steric hindrance imposed by the *tert*-butyl group of **16-S** and **16-Se**. Consequently, a molecule of **16-S** or **16-Se** cannot intercalate as deeply into the DNA helix as a molecule of **2-S** or **13-S** with sterically smaller methyl and *n*-propyl substituents, respectively. Consequently, **16-S** and **16-Se** will have a correspondingly larger displacement relative to the helix axis of ctDNA. If the relative propensities for intercalation and groove binding did not change with increasing dye concentration, then a linear increase in CD intensity with increasing concentration of dye would still be expected even with mixed binding.

Another explanation of the bisignate induced CD spectra might involve the existence of two electronic transitions at the 600-nm band with different transition moments. The specific orientation of each of these transition moments relative to the helix axis could result in the bisignate induced CD.

3. Summary and conclusions

While the literature describes compound **2-S** and related structures as intercalators of DNA, we have demonstrated that the chalcogenopyrylium dyes of this study (including **2-S**) have mixed binding modes to DNA. Results with the Topo I assay indicates that these dyes have some intercalative binding to DNA while competition dialysis assays suggest that other binding modes may be involved. Circular dichroism studies show a

pronounced induced CD and are consistent with intercalation of the dyes of this study producing bisignate CD spectra, which may reflect the distance of the dye from the central axis. These observations do not exclude the presence of other binding modes with the ratio of binding modes unchanged with increasing dye concentration. Values of K_b for these dyes are comparable whether determined by ITC or spectrophotometrically. This series of compounds represents a starting point for examining structure–activity studies for photoinactivation of viral and bacterial pathogens in blood.

4. Experimental

4.1. General methods

Solvents and reagents were used as received from Sigma–Aldrich Chemical Co. (St. Louis, MO) unless otherwise noted. 3-Methyl-1-butyne was purchased from GFS Chemical Inc. Concentration in vacuo was performed on a Büchi rotary evaporator. NMR spectra were recorded on a Varian Gemini-300 or Inova 500 instrument with residual solvent signal as internal standard: $CDCl_3$ (δ 7.26 for proton, δ 77.0 for carbon), CD_3OD (δ 3.31 for proton), CD_2Cl_2 (δ 53.8 for carbon). Infrared spectra were recorded on a Perkin-Elmer FT-IR instrument. UV-vis near-IR spectra were recorded on a Perkin-Elmer Lambda 12 spectrophotometer or on a Shimadzu UV-3600 spectrophotometer in quartz cuvettes with a 1-cm path length. CD spectra were recorded on JASCO-720 spectropolarimeter in quartz cuvettes with a 1-cm path length. Elemental analyses were conducted by Atlantic Microanalytical, Inc.

4.2. Materials

Poly(dAdT) and poly(dGdC) DNA sequences were obtained from Midland Certified Reagent Company (Midland, TX) as HPLC-purified and desalted products. To ensure optimal duplex formation, a buffered solution of each DNA sequence was heated to 90 °C and slowly cooled to room temperature (22–23 °C) before use. The resulting DNA duplexes ($[poly(dAdT)]_2$ and $[poly(dGdC)]_2$) were equilibrated in the appropriate buffer by dialyzing for at least 24 h before being used. Ultrapure calf thymus DNA was obtained from Invitrogen (Carlsbad, CA). Supercoiled pUC19 plasmid DNA (1.0 μg/μL) was purchased from Bayou Biolabs (Harahan, LA). DNA duplex concentrations (in bp) were determined spectrophotometrically using ε_{262} = 13,200 M^{-1} cm^{-1} for $[poly(dAdT)]_2$, ε_{256} = 16,800 M^{-1} cm^{-1} for $[poly(dGdC)]_2$ and ε_{260} = 12,824 M^{-1} cm^{-1} for calf thymus DNA. Purified human topoisomerase I enzyme was obtained from TopoGEN Inc. (Port Orange, FL). M13mp19 RF DNA was purchased from Life Technologies (Gaithersburg, MD).

4.3. General procedure for the addition of lithio alkynes to 4-dimethylaminophenyl propargyl aldehyde (3)

4.3.1. Preparation of 1-(4-dimethylaminophenyl)-1,5-hexadiyne-3-ol (4a). A solution of *n*-butyllithium (1.6 M, 4.13 mL, 6.6 mmol) in hexanes was added dropwise to a stirred solution of 1-propyne (0.24 g, 6.0 mmol) in anhydrous THF (30 mL) at −78 °C. After stirring for 0.5 h at −78 °C, the reaction mixture was warmed to 0 °C for an additional 0.5 h, and then was added via syringe to a solution of aldehyde **3**[14] (1.039 g, 6 mmol) in 10 mL of anhydrous THF at −78 °C. After stirring for 0.5 h, the solution was warmed to ambient temperature over a period of 1 h and saturated NH_4Cl solution (30 mL) was added. The reaction mixture was extracted with CH_2Cl_2 (3× 30 mL) and the combined organic layers were washed with water (30 mL), brine (30 mL), dried over sodium sulfate, and concentrated. The product was purified via chromatography on SiO_2 eluted with petroleum ether (pet ether)/EtOAc (3:1) to give alcohol **5a** as a yellow oil (1.02 g, 80%):. ^1H NMR [500 MHz, $CDCl_3$] δ 7.34 (AA′BB′, 2H, J = 9 Hz), 6.61 (AA′BB′, 2H, J = 9 Hz), 5.31 (d, 1H, J = 7 Hz), 2.97 (s, 6H), 2.16 (d, 1H, J = 7 Hz), 1.90 (s, 3H); ^{13}C NMR [300 MHz, $CDCl_3$] δ 150.3, 133.0, 111.6, 108.6, 85.2, 84.4, 81.0, 61.5, 53.0, 40.1, 3.7; IR (film, NaCl) 3583 cm^{-1}; HRMS (EI) *m/z* 213.1151 (calcd for $C_{14}H_{15}NO$: 213.1148).

4.3.2. 1-(4-Dimethylaminophenyl)hepta-1,4-diyn-3-ol (4b). ^1H NMR [500 MHz, $CDCl_3$] δ 7.34 (AA′BB′, 2H, J = 9 Hz), 6.61 (AA′BB′, 2H, J = 9 Hz), 5.33 (d, 1H, J = 7 Hz), 2.97 (s, 6H), 2.27 (q, 2H, J = 7.5 Hz), 2.265 (d, 1H, J = 7 Hz), 1.17 (t, 3H, J = 7.5 Hz); ^{13}C NMR [300 MHz, $CDCl_3$] δ 150.1, 132.7, 111.4, 108.5, 86.2, 84.8, 84.3, 76.4, 52.7, 39.9, 13.2, 12.2; IR (film, NaCl) 3391 cm^{-1}; HRMS (ESI) *m/z* 228.1383 (calcd for $C_{15}H_{17}NO + H^+$: 228.1383).

4.3.3. 1-(4-Dimethylaminophenyl)octa-1,4-diyn-3-ol (4c). ^1H NMR [500 MHz, $CDCl_3$] δ 7.33 (AA′BB′, 2H, J = 9 Hz), 6.61 (AA′BB′, 2H, J = 9 Hz), 5.34 (s, 1H), 2.969 (s, 6H), 2.24 (s, 1H), 2.235 (t, 2H, J = 7.5 Hz), 1.57 (sextet, 2H, J = 7.5 Hz), 1.00 (t, 3H, J = 7.5 Hz); ^{13}C NMR [300 MHz, $CDCl_3$] δ 150.5, 133.1, 111.8, 109.0, 85.2, 85.2, 84.8, 78.3, 53.1, 40.2, 21.9, 20.8, 13.6; IR (film, NaCl) 3392 cm^{-1}; HRMS (EI) *m/z* 241.1458 (calcd for $C_{16}H_{19}NO$: 241.1461).

4.3.4. 1-(4-Dimethylaminophenyl)-6-methylhepta-1,4-diyn-3-ol (4d). ^1H NMR [500 MHz, $CDCl_3$] δ 7.34 (AA′BB′, 2H, J = 8.5 Hz), 6.61 (AA′BB′, 2H, J = 8.5 Hz), 5.33 (d, 1H, J = 7.0 Hz), 2.97 (s, 6H), 2.63 (septet, 1H, J = 6.5 Hz), 2.19 (d, 1H, J = 7.0 Hz), 1.20 (d, 6H, J = 6.5 Hz); ^{13}C NMR [300 MHz, $CDCl_3$] δ 150.3, 132.9, 111.7, 108.8, 90.3, 85.0, 84.6, 77.1, 52.9, 40.1, 22.6, 20.4; IR: 3576 cm^{-1}; HRMS (ESI) *m/z* 242.1543 (calcd for $C_{16}H_{19}NO + H^+$: 242.1539).

4.3.5. 1-(4-Dimethylaminophenyl)nona-1,4-diyn-3-ol (4e). ^1H NMR [500 MHz, $CDCl_3$] δ 7.33 (AA′BB′, 2H, J = 9 Hz), 6.61 (AA′BB′, 2H, J = 9 Hz), 5.33 (s, 1H), 2.969 (s, 6H), 2.26 (t, 2H, J = 7.5 Hz), 2.257 (s, 1H), 1.53 (quintet, 2H, J = 7.5 Hz), 1.425 (sextet, 2H, J = 7.5 Hz), 0.92 (t, 3H, J = 7.5 Hz); ^{13}C NMR [300 MHz, $CDCl_3$] δ 150.4, 133.0, 111.8, 109.0, 85.4, 85.1, 84.8, 78.1, 53.1, 40.2, 30.5, 22.0, 18.5, 13.6; IR

(film, NaCl) 3581 cm^{-1}; HRMS (EI) *m/z* 255.1607 (calcd for $C_{17}H_{21}NO$: 255.1618).

4.3.6. 1-(4-Dimethylaminophenyl)-6,6-dimethylhepta-1,4-diyn-3-ol (4f). ^1H NMR [500 MHz, $CDCl_3$] δ 7.34 (AA′BB′, 2H, $J = 9$ Hz), 6.61 (AA′BB′, 2H, $J = 9$ Hz), 5.33 (s, 1H), 2.974 (s, 6H), 2.15 (s, 1H), 1.25 (s, 9H); ^{13}C NMR [300 MHz, $CDCl_3$] δ 150.3, 133.0, 111.7, 108.9, 93.2, 85.0, 84.73, 76.5, 53.1, 40.1, 30.7, 27.4; IR (film, NaCl) 3583 cm^{-1}; HRMS (EI) *m/z* 255.1607 (calcd for $C_{17}H_{21}NO$: 255.1618).

4.4. General procedure for the oxidation of 1-(4-dimethylaminophenyl)-1,4-diyn-3-ols

4.4.1. Preparation of 1-(4-(dimethylamino)phenyl)hexa-1,4-diyn-3-one (5a). Manganese dioxide (1.74 g, 20 mmol) was added to a solution of alcohol **4a** (711 mg, 3.3 mmol) in 20 mL of freshly distilled CH_2Cl_2 under an atmosphere of argon. The resulting mixture was heated at reflux for 4 h with stirring. The solution was then cooled to ambient temperature and filtered through a pad of Celite. The filtrate was washed with CH_2Cl_2 (3× 20 mL). The combined organic filtrates were concentrated. The residue was purified via recrystallization from hexane/THF (20:1) to give **5a** as red needles (0.57 g, 81%): mp 78–80 °C; ^1H NMR [500 MHz, $CDCl_3$] δ 7.50 (AA′BB′, 2H, $J = 9$ Hz), 6.63 (AA′BB′, 2H, $J = 9$ Hz), 3.04 (s, 6H), 2.09 (s, 3H); ^{13}C NMR [300 MHz, $CDCl_3$] δ 160.8, 151.9, 135.4, 111.4, 104.6, 95.6, 91.0, 89.9, 81.5, 39.8, 4.2; IR (KBr) 1591 cm^{-1}; HRMS (EI) *m/z* 211.0991 (calcd for $C_{14}H_{13}NO$: 211.0992).

4.4.2. 1-(4-Dimethylaminophenyl)hepta-1,4-diyn-3-one (5b). Yellow needles from hexane/THF(20:1), mp 70–72 °C; ^1H NMR [500 MHz, $CDCl_3$] δ 7.50 (AA′BB′, 2H, $J = 9$ Hz), 6.63 (AA′BB′, 2H, $J = 9$ Hz), 3.04 (s, 6H), 2.44 (q, 2H, $J = 8.5$ Hz), 1.25 (t, 3H, $J = 8.5$ Hz); ^{13}C NMR [300 MHz, $CDCl_3$] δ 161.06, 152.0, 135.5, 111.5, 104.9, 95.5, 95.1, 91.1, 81.7, 39.9, 12.9, 12.6; IR (KBr) 1591 cm^{-1}; HRMS (ESI) *m/z*: 226.1225 (calcd for $C_{15}H_{15}NO + H^+$: 226.1226).

4.4.3. 1-(4-Dimethylaminophenyl)octa-1,4-diyn-3-one (5c). ^1H NMR [500 MHz, $CDCl_3$] δ 7.49 (AA′BB′, 2H, $J = 9$ Hz), 6.62 (AA′BB′, 2H, $J = 9$ Hz), 3.04 (s, 6H), 2.40 (t, 2H, $J = 7$ Hz), 1.66 (sextet, 2H, $J = 7$ Hz), 1.048 (t, 3H, $J = 7$ Hz); ^{13}C NMR [300 MHz, $CDCl_3$] δ 160.9, 151.9, 135.4, 111.4, 104.6, 95.5, 94.0, 91.0, 82.4, 39.8, 21.1, 21.0, 13.4; IR (KBr) 1592 cm^{-1}; HRMS (EI) *m/z* 239.1303 (calcd for $C_{16}H_{17}NO$: 239.1305).

4.4.4. 1-(4-Dimethylaminophenyl)-6-methylhepta-1,4-diyn-3-one (5d). Red needles from hexanes, mp 74–76 °C; ^1H NMR [500 MHz, $CDCl_3$] δ 7.50 (AA′BB′, 2H, $J = 9$ Hz), 6.63 (AA′BB′, 2H, $J = 9$ Hz), 3.04 (s, 6H), 2.78 (sept, 1H, $J = 7$ Hz), 1.28 (d, 6H, $J = 7$ Hz); ^{13}C NMR [300 MHz, $CDCl_3$] δ 161.26, 151.9, 135.5, 111.5, 104.9, 98.6, 95.5, 91.1, 81.5, 39.9, 21.8, 20.9; IR: 1591 cm^{-1}; HRMS (ESI) *m/z* 240.1382 (calcd for $C_{16}H_{17}NO + H^+$: 240.1383).

4.4.5. 1-(4-Dimethylaminophenyl)nona-1,4-diyn-3-one (5e). ^1H NMR [500 MHz, $CDCl_3$] δ 7.47 (AA′BB′, 2H, $J = 9$ Hz), 6.61 (AA′BB′, 2H, $J = 9$ Hz), 3.02 (s, 6H), 2.42 (t, 2H, $J = 7.5$ Hz), 1.50 (quint, 2H, $J = 7.5$ Hz), 1.46 (sext, 2H, $J = 7.5$ Hz), 0.936 (t, 3H, $J = 7.5$ Hz); ^{13}C NMR [300 MHz, $CDCl_3$] δ 161.5, 152.5, 136.0, 112.0, 105.3, 96.2, 94.8, 91.7, 83.0, 40.4, 30.2, 22.5, 19.4, 14.0; IR (KBr) 1592 cm^{-1}; HRMS (EI) *m/z* 253.1450 (calcd for $C_{17}H_{19}NO$: 253.1461).

4.4.6. 1-(4-Dimethylaminophenyl)-6,6-dimethylhepta-1,4-diyn-3-one (5f). Yellow needles from hexane/THF (20:1), mp 103–105 °C; ^1H NMR [500 MHz, $CDCl_3$] δ 7.50 (AA′BB′, 2H, $J = 9$ Hz), 6.63 (AA′BB′, 2H, $J = 9$ Hz), 3.04 (s, 6H), 1.33 (s, 9H); ^{13}C NMR [300 MHz, $CDCl_3$] δ 161.3, 151.9, 135.5, 111.5, 105.0, 101.1, 95.4, 91.1, 81.0, 39.9, 30.0, 27.9; IR (KBr) 1591 cm^{-1}; HRMS (EI) *m/z* 253.1452 (calcd for $C_{17}H_{19}NO$: 253.1461).

4.5. General procedure for the conversion of 1,4-diyn-3-ones to chalcogenopyranones

4.5.1. Preparation of 2-(4-dimethylaminophenyl)-6-methyl-4H-thiopyran-4-one (6-S). A mixture of S (48 mg, 1.5 mmol), $NaBH_4$ (63 mg, 1.67 mmol), and 0.25 M NaOEt in EtOH (20 mL) was heated at reflux for 3 h under argon until the reaction turned clear. 1-(4-Dimethylaminophenyl)hexa-1,4-diyn-3-one **5a** (352 mg, 1.67 mmol) was added to 0.25 M NaOEt in EtOH (10 mL) and stirred for 1 h until the diynone was converted to a mixture of enol ethers as monitored by TLC. The solution of enol ethers was added to the reaction mixture and stirring was continued for 1 h. Water (30 mL) was added and the product was extracted with CH_2Cl_2 (3× 30 mL). The combined organic extracts were dried over $MgSO_4$, filtered and concentrated. The crude product was purified via column chromatography on SiO_2 eluted with EtOAc/pet ether (4:1) to give thiopyranone **6-S** as a yellow solid (0.19 g, 48%): mp 109–111 °C; ^1H NMR [500 MHz, $CDCl_3$] δ 7.49 (AA′BB′, 2H, $J = 9$ Hz), 7.07 (s, 1H), 6.78 (s, 1H), 6.73 (AA′BB′, 2H, $J = 9$ Hz), 3.04 (s, 6H), 2.42 (s, 3H); ^{13}C NMR [300 MHz, $CDCl_3$] δ 182.6, 153.3, 151.9, 150.1, 128.1, 127.5, 123.4, 122.9, 112.0, 40.1, 22.6; HRMS (ESI) *m/z* 246.0942 (calcd for $C_{14}H_{15}NOS + H^+$: 246.0947). Anal. Calcd for $C_{14}H_{15}NOS$: C: 68.54, H: 6.16, N: 5.71. Found: C, 68.18; H, 6.17; N, 5.54.

4.5.2. 2-(4-Dimethylaminophenyl)-6-ethyl-4H-thiopyran-4-one (7-S). mp 132–134 °C; ^1H NMR [500 MHz, $CDCl_3$] δ 7.50 (AA′BB′, 2H, $J = 9$ Hz), 7.07 (s, 1H), 6.81 (s, 1H), 6.73 (AA′BB′, 2H, $J = 9$ Hz), 3.035 (s, 6H), 2.69 (q, 2H, $J = 7.5$ Hz), 1.33 (t, 3H, $J = 7.5$ Hz); ^{13}C NMR [300 MHz, $CDCl_3$] δ 182.7, 156.6, 153.4, 151.9, 127.5, 126.5, 123.5, 123.0, 112.0, 40.0, 30.0, 14.1; HRMS (ESI) *m/z* 260.1098 (calcd for $C_{15}H_{17}NOS + H^+$: 260.1104). Anal. Calcd for $C_{15}H_{17}NOS$: C: 69.46, H: 6.61, N: 5.40. Found: C: 69.23; H, 6.66; N, 5.32.

4.5.3. 2-(4-Dimethylaminophenyl)-6-propyl-4H-thiopyran-4-one (8-S). mp 85–87 °C; ^1H NMR [500 MHz, $CDCl_3$] δ 7.495 (AA′BB′, 2H, $J = 9$ Hz), 7.08 (s, 1H),

6.80 (s, 1H), 6.72 (AA′BB′, 2H, J = 9 Hz), 3.03 (s, 6H), 2.62 (t, 2H, J = 7.5 Hz), 1.75 (sext, 2H, J = 7.5 Hz), 1.01 (t, 3H, J = 7.5 Hz); ^{13}C NMR [300 MHz, $CDCl_3$] δ 182.7, 155.1, 153.5, 151.9, 127.6, 127.4, 123.6, 123.1, 112.0, 40.1, 38.8, 23.1, 13.4; HRMS (ESI) m/z 274.1259 (calcd for $C_{16}H_{19}NOS + H^+$: 274.1260). Anal. Calcd for $C_{16}H_{19}NOS$: C, 70.29; H, 7.00; N, 5.12. Found: C, 69.99; H, 7.02; N, 4.95.

4.5.4. 2-(4-(Dimethylamino)phenyl)-6-isopropyl-4H-thiopyran-4-one (9-S). mp 100–102 °C; ^{1}H NMR [500 MHz, $CDCl_3$] δ 7.50 (AA′BB′, 2H, J = 9 Hz), 7.07 (s, 1H), 6.84 (s, 1H), 6.73 (AA′BB′, 2H, J = 9 Hz), 3.03 (s, 6H), 2.90 (sept, 1H, J = 7 Hz), 1.35 (d, 6H, J = 7 Hz); ^{13}C NMR [300 MHz, $CDCl_3$] δ 182.7, 161.9, 153.3, 151.8, 127.5, 125.0, 123.7, 123.1, 111.9, 40.0, 36.0, 28.8; HRMS (ESI) m/z 274.1257 (calcd for $C_{16}H_{19}NOS + H^+$: 274.1260). Anal. Calcd for $C_{16}H_{19}NOS$: C, 70.29; H, 7.00; N, 5.12. Found: C, 70.24; H, 6.96; N, 5.09.

4.5.5. 2-Butyl-6-(4-dimethylaminophenyl)-4H-thiopyran-4-one (10-S). mp 87–89 °C; ^{1}H NMR [500 MHz, $CDCl_3$] δ 7.50 (AA′BB′, 2H, J = 9 Hz), 7.08 (s, 1H), 6.80 (s, 1H), 6.73 (AA′BB′, 2H, J = 9 Hz), 3.03 (s, 6H), 2.65 (t, 2H, J = 7.5 Hz), 1.70 (quint, 2H, J = 7.5 Hz), 1.42 (sext, 2H, J = 7.5 Hz), 0.95 (t, 3H, J = 7.5 Hz); ^{13}C NMR [300 MHz, $CDCl_3$] δ 182.6, 155.4, 153. 4, 151.9, 127.5, 127.2, 123.5, 123.0, 112.0, 40.0, 36.5, 31.8, 21.9, 13.6; HRMS (ESI) m/z 288.1421 (calcd for $C_{17}H_{21}NOS + H^+$: 288.1417). Anal. Calcd for $C_{17}H_{21}NOS$: C: 71.04, H: 7.36, N: 4.87. Found: C, 70.97; H, 7.17; N, 4.87.

4.5.6. 2-*tert*-Butyl-6-(4-dimethylaminophenyl)-4H-thiopyran-4-one (11-S). mp 129–131 °C; ^{1}H NMR [500 MHz, $CDCl_3$] δ 7.52 (AA′BB′, 2H, J = 9 Hz), 7.09 (s, 1H), 6.97 (s, 1H), 6.74 (AA′BB′, 2H, J = 9 Hz), 3.04 (s, 6H), 1.40 (s, 9H); ^{13}C NMR [300 MHz, $CDCl_3$] δ 183.0, 165.1, 153.5, 151.8, 127.6, 124.7, 123.4, 123.1, 112.0, 40.0, 38.3, 30.5; HRMS (ESI) m/z 288.1419 (calcd for $C_{17}H_{21}NOS + H^+$: 288.1417). Anal. Calcd for $C_{17}H_{21}NOS$: C, 71.04; H, 7.36; N,: 4.87. Found: C, 70.94; H, 7.22; N, 4.86.

4.5.7. 2-*tert*-Butyl-6-(4-dimethylaminophenyl)-4H-selenopyran-4-one (11-Se). mp 108–110 °C; ^{1}H NMR [500 MHz, $CDCl_3$] δ 7.48 (AA′BB′, 2H, J = 8.5 Hz), 7.11 (s, 1H), 7.03 (s, 1H), 6.72 (AA′BB′, 2H, J = 8.5 Hz), 3.03 (s, 6H), 1.39 (s, 9H); ^{13}C NMR [300 MHz, $CDCl_3$] δ 185.2, 168.9, 155.5, 151.9, 127.8, 125.8, 125.1, 124.2, 112.0, 40.1, 39.4, 31.0; HRMS (ESI) m/z 336.0869 (calcd for $C_{17}H_{21}NO^{80}Se + H^+$: 336.0869). Anal. Calcd for $C_{17}H_{21}NOSe$: C, 61.07; H, 6.33; N, 4.19. Found: C, 60.94; H, 6.42; N, 4.28.

4.6. General procedure for preparing thiopyrylium and selenopyrylium dyes

4.6.1. Preparation of 2,4-di(4-dimethylaminophenyl)-6-methylthiopyrylium iodide (2-S). A mixture of 4-bromo-*N*,*N*-dimethylaniline (480 mg, 2.4 mmol) and Mg (88 mg, 3.6 mmol) was heated at reflux in THF (15 mL) for 2 h. A solution of **6-S** (147 mg, 0.60 mmol) in 10 mL of anhydrous THF was added dropwise to the reaction mixture and the resulting solution was heated at reflux for 1.0 h. The reaction mixture was cooled to 0 °C and 20 mL of 10% HI solution was added. The mixture was stirred for 1 h at 0 °C and was then extracted with CH_2Cl_2 (3× 20 mL). The combined organic extracts were washed with water (30 mL), brine (30 mL), dried over sodium sulfate, and concentrated. The solid was washed several times with ether, and dried in vacuo overnight to give **2-S** (212 mg, 74%): mp 216–218 °C; ^{1}H NMR [500 MHz, CD_3OD] δ 8.58 (s, 1H), 8.32 (s, 1H), 8.15 (AA′BB′, 2H, J = 9 Hz), 7.955 (AA′BB′, 2H, J = 9 Hz), 6.97 (AA′BB′, 2H, J = 9 Hz), 6.93 (AA′BB′, 2H, J = 9 Hz), 3.21 (s, 6H), 3.16 (s, 6H), 2.855 (s, 3H); ^{13}C NMR [300 MHz, $CDCl_3$] δ 162.5, 157.7, 155.9, 154.1, 153.5, 132.3, 129.3, 126.3, 121.6, 120.7, 120.2, 112.8, 112.5, 40.23, 4.17, 24.5; HRMS (ESI) m/z 349.1736 (calcd for $C_{22}H_{25}N_2S$: 349.1733); λ_{max} (CH_2Cl_2) 610 nm (ε 34,600 M^{-1} s^{-1}). Anal. Calcd for $C_{22}H_{25}N_2SI$: C, 55.46; H, 5.29; N, 5.88. Found: C, 55.13; H, 5.31; N, 5.79.

4.6.2. 2,4-Di(4-dimethylaminophenyl)-6-ethylthiopyrylium iodide (12-S). mp 225–227 °C; ^{1}H NMR [500 MHz, CD_3OD] δ 8.58 (s, 1H), 8.32 (s, 1H), 8.16 (AA′BB′, 2H, J = 9 Hz), 7.96 (AA′BB′, 2H, J = 8.5 Hz), 6.97 (AA′BB′, 2H, J = 8.5 Hz), 6.93 (AA′BB′, 2H, J = 9 Hz), 3.21 (s, 6H), 3.17 (q, 2H, J = 7.5 Hz), 3.16 (s, 6H), 1.50 (t, 3H, J = 7.5 Hz); ^{13}C NMR [300 MHz, CD_2Cl_2] δ 165.4, 164.2, 157.2, 154.9, 154.4, 132.0, 129.5, 125.7, 122. 3, 121.7, 121.4, 113.2, 112.9, 40.5, 40.4, 31.9, 15.4; HRMS (ESI) m/z 363.1884 (calcd for $C_{23}H_{27}N_2S$: 363.1889); λ_{max} (CH_2Cl_2) 609 nm (ε 48,600 M^{-1} s^{-1}). Anal. Calcd for $C_{23}H_{27}IN_2S$: C, 56.33; H, 5.55; N, 5.71. Found: C, 56.10; H, 5.69; N, 5.50.

4.6.3. 2,4-Di(4-dimethylaminophenyl)-6-propylthiopyrylium iodide (13-S). mp 227–229 °C; ^{1}H NMR [500 MHz, CD_3OD] δ 8.60 (s, 1H), 8.32 (s, 1H), 8.16 (AA′BB′, 2H, J = 9 Hz), 7.965 (AA′BB′, 2H, J = 9 Hz), 6.975 (AA′BB′, 2H, J = 9 Hz), 6.94 (AA′BB′, 2H, J = 9 Hz), 3.21 (s, 6H), 3.165 (s, 6H), 3.12 (t, 2H, J = 7.5 Hz), 1.92 (sext, 2H, J = 7.5 Hz), 1.11 (t, 3H, J = 7.5 Hz); ^{13}C NMR [300 MHz, CD_2Cl_2] δ 164.3, 164.1, 157.1, 154.8, 154.2, 132.0, 129.6, 126.3, 122.6, 122.3, 121.9, 113.5, 113.3, 40.7, 40.22, 30.0, 24.9, 13.6; HRMS (ESI) m/z 377.2044 (calcd for $C_{24}H_{29}N_2S$: 377.2046); λ_{max} (CH_2Cl_2) 609 nm (ε 74,400 M^{-1} s^{-1}). Anal. Calcd for $C_{24}H_{29}IN_2S$: C, 57.14; H, 5.79; N, 5.55. Found: C, 57.11; H, 5.61; N, 5.50.

4.6.4. 2,4-Di(4-(dimethylamino)phenyl)-6-isopropylthiopyrylium iodide (14-S). mp > 300 °C; ^{1}H NMR [500 MHz, CD_3OD] δ 8.59 (s, 1H), 8.31 (s, 1H), 8.16 (AA′BB′, 2H, J = 9 Hz), 7.97 (AA′BB′, 2H, J = 9 Hz), 6.975 (AA′BB′, 2H, J = 9 Hz), 6.94 (AA′BB′, 2H, J = 9 Hz), 3.48 (septet, 1H, J = 7 Hz), 3.21 (s, 6H), 3.16 (s, 6H), 1.54 (d, 6H, J = 7 Hz); ^{13}C NMR [300 MHz, CD_2Cl_2] δ 170.7, 164.1, 157.2, 154.8, 154.4, 131.9, 129.5, 124.3, 122.4, 122.0, 121.5, 113.2, 112.9, 40.5, 40.4, 38.1, 23.7; HRMS (ESI) m/z 377.2045 (calcd for $C_{24}H_{29}N_2S$: 377.2046); λ_{max} (CH_2Cl_2) 607 nm (ε 50,900 M^{-1} s^{-1}). Anal. Calcd for $C_{24}H_{29}IN_2S$: C, 57.14; H, 5.79; N, 5.55. Found: C, 56.83; H, 5.71; N, 5.18.

4.6.5. 2-Butyl-4,6-di(4-dimethylaminophenyl)thiopyrylium iodide (15-S). mp 228–230 °C; ^{1}H NMR [500 MHz, CD_3OD] δ 8.58 (s, 1H), 8.32 (s, 1H), 8.16 (AA′BB′, 2H, J = 9 Hz), 7.96 (AA′BB′, 2H, J = 9 Hz), 6.97 (AA′BB′, 2H, J = 9 Hz), 6.94 (AA′BB′, 2H, J = 9 Hz), 3.21 (s, 6H), 3.14 (s, 6H), 3.14 (t, 2H, J = 7.5 Hz), 1.87 (quint, 2H, J = 7.5 Hz), 1.53 (sext, 2H, J = 7.5 Hz), 1.03 (t, 3H, J = 7.5 Hz); ^{13}C NMR [300 MHz, CD_2Cl_2] δ 164.4, 164.2, 157.1, 154.7, 154.1, 132.0, 129.6, 126.2, 122.7, 122.1, 122.0, 113.6, 113.5, 4.73, 38.2, 33.6, 22.5, 13.8; HRMS (ESI) m/z 391.2206 (calcd for $C_{25}H_{31}N_2S$: 391.2202); λ_{max} (CH_2Cl_2) 609 nm (ε 63,600 M^{-1} s^{-1}). Anal. Calcd for $C_{25}H_{31}IN_2S$: C, 57.91; H, 6.03; N, 5.40. Found: C, 57.53; H, 6.22; N, 5.32.

4.6.6. 2-*tert*-Butyl-4,6-di(4-dimethylaminophenyl)thiopyrylium iodide (16-S). mp > 300 °C; ^{1}H NMR [500 MHz, CD_3OD] δ 8.585 (s, 1H), 8.32 (s, 1H), 8.145 (AA′BB′, 2H, J = 9.5 Hz), 7.98 (AA′BB′, 2H, J = 9 Hz), 6.98 (AA′BB′, 2H, J = 9 Hz), 6.94 (AA′BB′, 2H, J = 9 Hz), 3.21 (s, 6H), 3.16 (s, 6H), 1.62 (s, 9H); ^{13}C NMR [300 MHz, CD_2Cl_2] δ 173.9, 164.3, 157.3, 154.8, 154.5, 131.7, 129.7, 123.3, 122.7, 121.8, 121.6, 113.2, 112.9, 40.8, 40.5, 40.4, 31.2; HRMS (ESI) m/z 391.2206 (calcd for $C_{25}H_{31}N_2S$: 391.2202); λ_{max} (CH_2Cl_2) 605 nm (ε 69,900 M^{-1} s^{-1}). Anal. Calcd for $C_{25}H_{31}IN_2S$: C, 57.91; H, 6.03; N, 5.40. Found: C, 58.08; H, 5.99; N, 5.37.

4.6.7. 2-*tert*-Butyl-4,6-di(4-dimethylaminophenyl)selenopyrylium iodide (16-Se). mp > 300 °C; ^{1}H NMR [500 MHz, CD_3OD] δ 8.45 (s, 1H), 8.27 (s, 1H), 8.12 (AA′BB′, 2H, J = 8 Hz), 7.94 (AA′BB′, 2H, J = 8 Hz), 6.98 (AA′BB′, 2H, J = 8 Hz), 6.93 (AA′BB′, 2H, J = 8 Hz), 3.19 (s, 6H), 3.16 (s, 6H), 1.62 (s, 9H); ^{13}C NMR [300 MHz, CD_2Cl_2] δ 181.8, 171.8, 157.9, 154.7, 154.7, 131.9, 130.1, 124.8, 124.3, 124.2, 122.4, 113.3, 113.2, 42.1, 40.6, 40.5, 31.8; HRMS (ESI) m/z 439.1657 (calcd for $C_{25}H_{31}N_2{}^{80}Se$: 439.1652); λ_{max} (CH_2Cl_2) 619 nm (ε 52,900 M^{-1} s^{-1}). The iodide was converted to the chloride with Amberlite IRA-400 Chloride ion exchange resin as described above to give **16-Se** as the chloride salt, mp 251–253 °C. Anal. Calcd for $C_{25}H_{31}ClN_2Se$: C, 63.36; H, 6.59; N, 5.91. Found: C, 63.08; H, 6.23; N, 5.93.

4.7. Determination of partition coefficients

The octanol/water partition coefficients were measured using UV–vis spectrophotometry. The measurements were done using a 'shake flask' direct measurement.[26] Mixing for 1 h was followed by 4 h of settling time. Equilibration and measurements were made at 23 °C using a Perkin-Elmer Lambda 12 spectrophotometer. HPLC-grade 1-octanol was obtained from Sigma–Aldrich. Deionized water was used.

4.8. Determination of binding constants to DNA

4.8.1. Spectrophotometric determination of binding constants. The binding constants of thiopyrylium dyes to covalently closed supercoiled doubled-stranded DNA (using the genome from M13mp19) and to calf thymus DNA were determined by absorption (spectrophotometric) titration at room temperature using a constant concentration for each dye (ranging from 7.5×10^{-5} to 1.5×10^{-6} M, depending on the dye) and DNA concentrations ranging from 0 to 2.1×10^{-4} M in buffer (0.1 M NaCl, 0.01 M Tris, 0.001 M EDTA, pH 7.4 for M13mp19 DNA; and 0.006 M Na_2HPO_4, 0.002 M NaH_2PO_4, 0.001 M Na_2EDTA, and 0.185 M NaCl, pH 7.0 for ctDNA). The binding constant, K_b, was determined from the absorption changes during the DNA titration and was calculated using the equation $(\varepsilon_b - \varepsilon_f)/(\varepsilon_a - \varepsilon_b) = (1/K_b) \times (1/[DNA]) + 1$, where ε_a, ε_f and ε_b are the molar extinction coefficients for the apparent absorption of the complex at a given DNA concentration, for the dye free in solution, and for the dye fully bound to DNA, respectively. The value of ε_b was determined from the titration where further addition of DNA did not result in changes to the spectrum. The binding constant for each dye was determined by plotting $(\varepsilon_b - \varepsilon_f)/(\varepsilon_a - \varepsilon_b)$ versus (1/[DNA]), and K_b was obtained as the reciprocal value of the slope[24,25] of the best fit line passing through an intercept of 1. Linear regressions of data were performed using commercial software (InStat, GraphPad, San Diego, CA).

4.8.2. Binding constants to DNA determined by isothermal titration calorimetry (ITC). Calorimetric titrations were carried out on a MicroCal VP-ITC (MicroCal Inc., Northampton, MA). The data were analyzed using the Origin 7.0 software provided by the manufacturer. All experiments were run at 25 °C in MES00 buffer (1×10^{-2} M MES (2(*N*-morpholino)ethanesulfonic acid) containing 1×10^{-3} M EDTA, with the pH adjusted to 6.25 with NaOH). Exactly 15 μL of the drug solution (1.6×10^{-4} M) was injected into a buffered solution of ctDNA (1.5×10^{-5} M in bp, 1.4 mL) over 25 s at 240-s intervals using a 250-μL syringe rotating at 290 rpm. Samples were degassed at 20 °C using a ThermoVac apparatus (MicroCal) before use. Each peak corresponded to the decrease in the power supplied to keep the temperatures of the sample and reference cells the same for each injection and represents the heat given off. In each case, response signals were corrected for the small heat of dilution associated with titrating the drug solution into the buffer. The heat of dilution for titrating buffer into DNA was found to be negligible. The heat released upon binding was directly proportional to the amount of binding that occurred. A binding isotherm of heat released as a function of the drug/DNA molar ratio was constructed and the data fitted by nonlinear least square fitting analysis to a model based on a single set of identical binding sites.

4.9. Competition dialysis assay

For each dialysis run, exactly 1000 μL (100 μM in bp) of $[poly(dAdT)]_2$ and $[poly(dGdC)]_2$ was placed inside separate Spectra/Por DispoDialyzer membranes/bags (MWCO = 8000 Da, Spectrum) and dialyzed against 300 mL (5 μM) of a common compound solution in 0.05 M sodium phosphate buffer, pH 7.0. Dialysis experiments were allowed to equilibrate for 24 h with constant stirring at room temperature. After dialysis, the

content of each DispoDialyzer bag was removed and the requisite amount of sodium dodecyl sulfate (SDS) solution added to make the final SDS content equal to 1% w/v (this serves to dislodge the compound from the DNA). The amount of compound that was bound to each DNA sequence was then determined spectrophotometrically (given by the total compound concentration in each bag minus the free compound concentration in the dialysate solution outside the membrane). The relative concentrations of compound bound to each DNA sequence gives a direct measure of binding preferences. Dialysis experiments were repeated and the two sets of results averaged. Concentrations of compound were quantified using the following maxima and extinction coefficients in water: For **2-S**, λ_{max} 594 nm (ε 27,000 $M^{-1}\,cm^{-1}$); For **2-Se**, λ_{max} 623 nm (ε 37,000 $M^{-1}\,cm^{-1}$); For **13-S**, λ_{max} 594 nm (ε 49,000 $M^{-1}\,cm^{-1}$); For **16-S**, λ_{max} 595 nm (ε 35,000 $M^{-1}\,cm^{-1}$); For **16-Se**, λ_{max} 623 nm (ε 46,000 $M^{-1}\,cm^{-1}$).

4.10. Topoisomerase I DNA unwinding assay

Typically, 2.4×10^{-7} g of supercoiled pUC19 plasmid DNA was incubated with 5 U of human topoisomerase I (Topo I) enzyme for 5 min at 37 °C in 1× Topo I reaction buffer. The appropriate amount of compound was then added and the reaction mixture incubated for a further 1 h at 37 °C. The reaction was terminated using 0.5% SDS and 5×10^{-4} g/mL proteinase K. Subsequent incubation for an additional 15 min was followed by enzyme and compound extraction using a mixture of phenol/chloroform/isoamyl alcohol (25:24:1). The remaining DNA sample was then run on an agarose gel (1%) at 75 V for 3 h, stained with ethidium bromide and photographed (type 667 film).

In the Topo I assay, Bands I and II represent the supercoiled and relaxed plasmid DNA, respectively. [Note that ''supercoiled'' pUC19 plasmid preparations normally contain a small proportion of nicked/relaxed DNA (see control lane with no Topo I or drug treatment)]. In the presence of Topo I and absence of drug, the supercoiled plasmid DNA is relaxed (Band II) by the enzyme. When the DNA is then exposed to increasing drug concentration, drug-induced DNA unwinding will create positive supercoils since the DNA was pre-relaxed by Topo I. However, in the face of excess Topo I enzyme, the positive supercoils will be removed recreating relaxed DNA [Note that we incubate 5 U of Topo I for 1 h, which is more than 5 times the amount of enzyme (and twice the incubation time) suggested by the manufacturer for complete relaxation of the amount of DNA used in our studies; this should be more than adequate to compensate for any inhibitory effects]. The Topo I enzyme catalyzes relaxation by changing the DNA linking number (L_k). Upon drug removal(phenol:$CHCl_3$ extraction) and Topo I inactivation and (proteinase K treatment), the DNA re-supercoils due to its altered L_k, and does so to the extent to which L_k was changed. In our experiments, drug concentrations are increased until maximum re-supercoiling of the DNA occurs (Band I), that is, compared to the control lane (lane 1).

4.11. Ethidium bromide displacement assay

A solution of ethidium bromide (ETBr, 5×10^{-6} M, 1.4 mL) was pre-incubated with calf thymus DNA (1×10^{-5} M, 1.4 mL) at room temperature (22–23 °C) for 30 min in MES00 buffer, pH 6.3. Aliquots of exactly 3 μL of the chalcogenopyrylium compound (1×10^{-4} M) were then titrated into the ETBr-DNA solution (2.8 mL) and the change in fluorescence measured, after 5 min incubation periods, using a FluoroMax-2 fluorometer (Horiba Jobin Yvon-Spex, excitation 545 nm and emission 595 nm). The addition of 3 μL aliquots was continued until the DNA was saturated (i.e., no further change in fluorescence due to EtBr displacement).[22] Control experiments showed that the thiopyrylium dyes (free or DNA-bound) had no significant background fluorescence at the excitation (545 nm) and emission (595 nm) wavelengths of EtBr.

Acknowledgements

R.E.M. thanks Dr. Ben Miller at the University of Rochester Medical Center for access to the ITC equipment, Mr. James Keyes for technical assistance in the competition dialysis experiments, and the National Science Foundation (DUE Grant #0436298) and the Geneseo Foundation for partial support of this work.

References and notes

1. Dodd, R. Y.; Notari, E. P.; Stramer, S. L. *Transfusion* **2002**, *42*, 975.
2. Detty, M. R.; Gibson, S. L.; Wagner, S. J. *J. Med. Chem.* **2004**, *47*, 3897.
3. Wagner, S. J. *Transfus. Med. Rev.* **2002**, *16*, 61.
4. Wagner, S. J.; Skripchenko, A.; Robinette, D.; Foley, J. W.; Cincotta, L. *Photochem. Photobiol.* **1998**, *67*, 343.
5. OhUigin, C.; McConnell, D. J.; Kelly, J. M.; van der Putten, W. J. *Nucleic Acids Res.* **1987**, *15*, 7411.
6. Stockert, J. C.; Del Castillo, P. *Histochemistry* **1989**, *91*, 263.
7. Hagmar, P.; Pierrou, S.; Nielsen, P.; Norden, B.; Kubista, M. *J. Biomol. Struct. Dyn.* **1992**, *9*, 667.
8. Mohammad, T.; Morrison, H. *Bioorg. Med. Chem. Lett.* **1999**, *9*, 2249.
9. Yamamoto, N.; Okamoto, T.; Kawaguchi, M. *Nucleic Acids Symp. Ser.* **1993**, *29*, 83.
10. Wagner, S. J.; Skripchenko, A.; Cincotta, L.; Thompson-Montgomery, D.; Awatefe, H. *Transfusion* **2005**, *45*, 752.
11. Reynolds, G. A. *Synthesis* **1975**, *10*, 638.
12. Wizinger, von R.; Grune, A.; Jacobi, E. *Helv. Chim. Acta* **1956**, *39*, 1.
13. Detty, M. R.; Murray, B. J. *J. Org. Chem.* **1982**, *47*, 5235.
14. Brennan, N. K.; Hall, J. P.; Davies, S. R.; Gollnick, S. O.; Oseroff, A. R.; Gibson, S. L.; Hilf, R.; Detty, M. R. *J. Med. Chem.* **2002**, *45*, 5123.
15. Leonard, K.; Nelen, M.; Raghu, M.; Detty, M. R. *J. Heterocycl. Chem.* **1999**, *36*, 707.
16. (a) Anderson, C. F.; Record, M. T., Jr.; Hart, P. A. *Biophys. Chem.* **1978**, *7*, 301; (b) Lohman, T. M.; deHaseth, P. L.; Record, M. T., Jr. *Biophys. Chem.* **1978**, *8*, 281; (c) Record, M. T., Jr.; Anderson, C. F.; Lohman, T. M. *Q. Rev. Biophys.* **1978**, *11*, 102.

17. Pommier, Y.; Covey, J. M.; Kerrigan, D.; Markovits, J.; Pham, R. *Nucleic Acids Res.* **1987**, *15*, 6713.
18. Dziegielewski, J.; Slusarski, B.; Konitz, A.; Skladanowski, A.; Konopa, J. *Biochem. Pharmacol.* **2002**, *63*, 1653.
19. McKnight, R. E.; Gleason, A. B.; Keyes, J. A.; Sahabi, S. *Bioorg. Med. Chem. Lett.* **2007**, *17*, 1013.
20. Ren, J.; Chaires, J. B. *Biochemistry* **1999**, *38*, 16067.
21. Tanious, F. A.; Veal, J. M.; Buczak, H.; Ratmeyer, L. S.; Wilson, W. D. *Biochemistry* **1992**, *31*, 3103.
22. Boger, D. L.; Fink, B. E.; Brunette, S. R.; Tse, W. C.; Hedrick, M. P. *J. Am. Chem. Soc.* **2001**, *123*, 5878–5891.
23. Lee, C. H.; Chang, C.-T.; Wetmur, J. G. *Biopolymers* **1973**, *12*, 1099.
24. Tuite, E.; Nordén, B. *J. Am. Chem. Soc.* **1994**, *116*, 7548.
25. (a) Lyng, R.; Hird, T.; Nordén, B. *Biopolymers* **1987**, *26*, 1327; (b) Lyng, R.; Rodger, A.; Nordén, B. *Biopolymers* **1991**, *31*, 1709; (c) Lyng, R.; Rodger, A.; Nordén, B. *Biopolymers* **1992**, *32*, 1201.
26. Sangster, J. In *Octanol–Water Partition Co-efficients: Fundamentals and Physical Chemistry*; Fogg, P. G. T., Ed.; John Wiley and Sons: New York, 1997.